Received: 4 September 2022 | Revised: 11 April 2023 | Accepted: 8 May 2023
DOI: 10.1002/fam.3153

RESEARCH ARTICLE

WILEY

# A theoretical evaluation of the impact of the type of reaction on heat production and material losses in biomass piles

**Sixten Dahlbom**[1] | **Erik Anerud**[2] | **Anders Lönnermark**[1] | **Mohit Pushp**[1]

[1]Division Safety and Transport, Fire and Safety Department, RISE Research Institute of Sweden, Borås, Sweden

[2]Department of Biomaterials and Technology, Swedish University of Agricultural Science, Forest Biomaterials and Technology, Umeå, Sweden

**Correspondence**
Sixten Dahlbom, Division Safety and Transport, Fire and Safety Department, RISE Research Institute of Sweden, Box 857, 501 15, Borås, Sweden.
Email: sixten.dahlbom@ri.se

**Funding information**
AFA Försäkring; Energimyndigheten

## Abstract

Self-heating during storage of biomass in piles causes material losses, leads to emissions to air, and poses a risk of fire. There are different techniques to assess a biomass material's propensity for self-heating, some of these are briefly reviewed. One of these techniques is isothermal calorimetry, which measures thermal power from materials and produces time-resolved curves. A recently developed and published test standard, ISO 20049-1:2020, describes how the self-heating of pelletized biofuels can be determined by means of isothermal calorimetry and how thermal power and the total heat produced during the test should be measured by isothermal calorimetry. This paper supports interpretation of the result obtained by isothermal calorimetry; the mentioned standard provides examples of peak thermal power and total heat but does not provide any assistance on how the result from isothermal measurements should be interpreted or how the result from measurements on different samples could be compared. This paper addresses the impact of different types of reactions, peak thermal power, total heat released (heat of reaction), activation energy, heat conductivity, and pile size on the temperature development in a generic pile of biomass. This paper addresses important parameters when the result from isothermal calorimetry is evaluated. The most important parameter, with respect to temperature development in large piles, was found to be the total heat released. It was also proposed that safe storage times, that is, the time until a run-away of the temperature in the pile, could be ranked based on the time to the peak thermal power.

KEYWORDS
biomaterial, isothermal calorimetry, reactivity, self-heating, storage

## 1 | INTRODUCTION

### 1.1 | Self-heating and its implications on the industry

Storage of biomass (e.g., wood chips, bark, and pellets) in large piles or as pellets in a silo lead, due to complex combinations of biological, physical, and chemical processes, to dry matter losses.[1] Such processes include the decomposition of unstable products, biological activity, and physical and chemical oxidation. Dry matter losses (estimated to an annual loss corresponding to 3 TWh in Sweden) lead to gaseous emissions and self-heating,[2] which pose a risk of self-ignition if produced heat is not sufficiently dissipated.[3] Processes for self-heating coincide, and biological, chemical, or physical processes can interact and accelerate each other. The temperature and off-gassing during storage reflect the combined exothermic reactions, and increased temperature is equated to increased gaseous emissions and accelerated dry matter degradation.[4] Degradation and self-heating processes are substrate-dependent and influenced by material properties, that is, particle size distribution, moisture content, and storage volume.[5] During storage of comminuted unprocessed biomass, microbial activity is the most predominant initial mechanism for the deterioration at temperatures below 50°C. However, once the temperature reaches approximately 70°C, most of the fungi die,[6] and physical–chemical oxidation processes, which were accelerated by the microbial processes, become the dominating process for self-heating. The risk of extensive degradation and self-heating during storage can be minimised by measures to impair microbial access to readily available nutrients and moisture by increasing target chip size, reducing the number of fine particles,[7–9] by sieving or by protecting the biomass from rewetting by precipitation[10–13] (by covering it). The properties of the material used for covering the piles affect the self-heating processes; materials that protect the biomass from moisture and simultaneously enable hot water vapor to leave the pile are preferable.[14] The main difference with the storage of pellets is that biomass is processed, homogenous and dry, which reduces the risk of spontaneous self-heating and self-ignition compared to unpressed biomass.[15] However, pellets are hydrophilic and even if stored in air tight silos, auto-oxidative processes may increase the temperature to 60°C,[16,17] but the process may be slowed or delayed if an antioxidant is present in the material.[18]

Studies of Swedish statistics of firefighting operation[19,20] show that the number of fires in industrial biomass and waste facilities is relatively constant over the years, around 200 fires annually in Sweden. The studies included biomass and waste facilities, but also the fires at waste facilities in many cases involve stored biomass, for example, wood chips and bark. For the fires, self-heating/autoignition was registered as the source of ignition in most cases (45%–65% for fires not in buildings), with "Unknown" as the second most frequent reason.[19,20] The above-mentioned statistics together with results from a questionnaire survey (for facility representatives) suggest that the total amount of burnt and damaged material during fires at biomass or waste facilities in Sweden each year is 6500–7500 metric tonnes.[19] The total cost for the fires during a year were estimated to 150–350 MSEK, but then it should be noted that costs for emissions to the environment are not estimated nor included.

## 1.2 | Methods to assess biomass' self-heating propensity

Because of the fire risk and the large costs associated with fire, different techniques and models have been developed to estimate and compare the reactivity of different materials. Some of the methods are based on the Frank-Kamenetskii theory. These methods involve tests where a wire mesh basket is filled with the material under investigation. The basket is placed in an oven with a set temperature. If the ignition criterion is met, the test is repeated at a lower temperature, otherwise, the set temperature is increased. The aim of this procedure is to find the self-ignition temperature (SIT), which is defined as the lowest temperature where ignition occurs. Other methods to investigate the reactivity of materials are thermogravimetric analysis (TGA) and differential scanning calorimetry (DSC). However, these two methods are limited by the size of the test sample and the sensitivity of the instrument. As an alternative approach, a method based on isothermal calorimetry was developed.[21] In this method, sample sizes in the gram scale are proposed to be used. The applicability of isothermal calorimetry as a method to estimate the risk of self-heating with following self-ignition has been demonstrated by Larsson et al.[22] The researchers measured thermal power from 31 different biomass pellet batches and, based on the specific peak thermal power ($HRR_{max}$), they ranked the pellets' reactivity. Three categories of reactivity (high, intermediate, and low reactivity) were used; pellets with a specific peak thermal power ≥0.61 mW/g were classified as high reactive.

In a study on heat production in municipal waste,[23] the authors used isothermal calorimetry and compared different samples' reactivity by the time to reach a total heat of 40 J for approximately the same sample mass (0.5 g). For their material and purpose, authors argued that 40 J was the best trade-off between uncertainties in measurements of the thermal power and oxygen depletion in the ampoules.

The test-standard ISO 20049-1:2020 describes how the self-heating of pelletized biofuels can be determined by means of isothermal calorimetry[24] and how the first peak in thermal power and the total heat produced during the test (24 h) should be measured by isothermal calorimetry. The standard provides examples of peak thermal power and total heat but does not provide any assistance on how the result from isothermal measurements should be interpreted.

The three presented methods to assess the propensity for self-heating (specific peak thermal power, specific total heat, and the time to reach a certain specific total heat) use numbers that are easily accessible from isothermal measurements. However, it has never been discussed if or how the type of reaction, that is, the thermal power versus time as revealed by isothermal calorimetry, or how reactions' temperature dependencies will affect the self-heating of the material when stored in piles. The scope of this study is to illustrate how the reactions taking place more accurately can be addressed to compare the reactivity of different materials, that is, the risk of self-ignition or loss of material. This will be achieved through the modeling of a generic pile. Figure 1 shows measurements of thermal power from bark samples at 50°C. The figure illustrates the complexity of comparing different materials' reactivity. Some materials show very early peaks in thermal power, one material shows an initial peak, and a secondary peak after 75 h, and some materials show almost constant thermal power at certain time intervals.

# 2 | DEFINITIONS AND HEAT BALANCE EQUATION

## 2.1 | Definition of the generic pile

To select the properties of the generic pile used in the modeling, a review of published data on biomass properties was made; a summary of the review is given in Table 1. Most of the data were found either

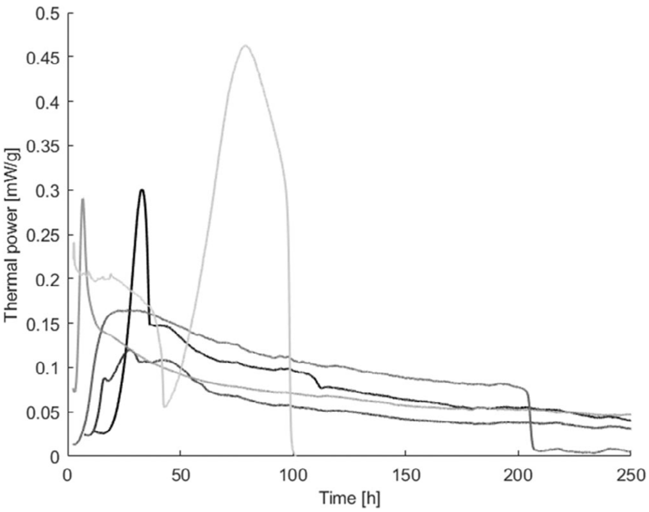

**FIGURE 1** Thermal power versus time for bark samples at 50°C. The sudden drops in thermal power at 95 and 205 h are probably due to oxygen depletion in the ampoulles.

directly in a study by Krigstin et al.[25] or in references cited by that study. The authors compared self-heating in bark and woodchip biomass piles and investigated the impact from different parameters, for example, initial moisture content, pile length, specific heat, etc. One of the cited sources is a study by Larsson et al.,[26] which was part of a larger project that aimed at increasing safety during the storage of biomass pellets. Based on the literature review (cf. Table 1), it was decided to use the following parameters to define the properties of the generic pile:

- Bulk density: 300 kg/m[3]
- Bulk heat capacity: 1470 J/kg/K
- Bulk thermal conductivity: 0.11 W/m/K
- Apparent activation energy: 97 kJ/mol
- Heat of reaction: 80 J/g
- Pile size: 45 × 15 × 6 m (with the shape of a rectangular cuboid, cf. Figure 2)

## 2.2 | Kinetic and reaction model

The rate of a chemical or biological reaction can be described by a kinetic model, as in Equation 1. The kinetic model is defined as a product of the reaction constant (with its temperature dependency described by the Arrhenius equation) and the reaction model. In other words, the rate of the reaction at different temperatures times the reaction rate at different extents of reaction.

$$\frac{d\alpha}{dt} = k(T)\cdot f(\alpha) = Ae^{\frac{-E_a}{RT}}\cdot f(\alpha) \tag{1}$$

where $A$ is the pre-exponential factor, $E_a$ is the apparent activation energy, R is the gas constant, $T$ is the temperature, α is the extent of the reaction, and f(α) is the reaction model. The reaction model describes how the reaction proceeds and depends, among other factors, on the material and concentration(s) of reactant(s). The temperature dependency is reflected by the kinetic model, but is not part of the reaction model. The reaction model needs to be selected and the kinetic parameters adjusted to match the material under investigation and cannot be generalized. To evaluate the impact on the self-heating of different reaction models, four different reaction models were selected. The selection was made to cover different types of apparent reactions, as revealed by isothermal calorimetry. The first reaction model (RM1) is given in Equation 2 and reflects a constant reaction rate, that is, a zeroth order reaction. The second reaction model (RM2), given in Equation 3, describes a first-order reaction, that is, the reaction rate decreases exponentially when the reactant is consumed. RM2 is a reaction model that, in general terms, well describes the reaction rate of biomass pellets. The third reaction model (RM3) is Ng's reaction model[32] with exponents equal to unity, compare Equation 4. Özilgen and Özilgen[33] demonstrated how this model could be applied to lipid oxidation. Self-heating of wood pellets has previously been attributed to fatty acids,[18] and this reaction model could therefore be considered representable of self-heating of biomass. The fourth reaction model (RM4) is an extension of RM3, that is Ng's reaction model without limitations on the exponents. The exponents in RM4 (Equation 5) were empirically selected to give a reaction model somewhere in between RM2 and RM3.

$$f(\alpha) = 1 \tag{2}$$

$$f(\alpha) = C_0\cdot(1-\alpha) \tag{3}$$

$$f(\alpha) = \alpha\cdot(1-\alpha) \tag{4}$$

$$f(\alpha) = \alpha^{0.4}\cdot(1-\alpha)^{2.2} \tag{5}$$

## 2.3 | Heat balance equation and physical parameters

The overall heat balance, expressed in three-dimensional coordinates is given in Equation 6. By assuming no variation in temperature in the z-direction, the problem reduces to two dimensions, that is, the cross directions, as described by Equation 7 and as illustrated in Figure 2.

$$\rho C_p\frac{\partial T}{\partial t} = \lambda\left(\frac{\partial^2 T}{\partial x^2}+\frac{\partial^2 T}{\partial y^2}+\frac{\partial^2 T}{\partial z^2}\right)+\dot{q}_r \tag{6}$$

$$\rho C_p\frac{\partial T}{\partial t} = \lambda\left(\frac{\partial^2 T}{\partial x^2}+\frac{\partial^2 T}{\partial y^2}\right)+\dot{q}_r \tag{7}$$

where $\rho$ is the bulk density, $C_p$ is the specific heat capacity, and $\lambda$ is the bulk thermal conductivity. $\dot{q}_r$ denotes the rate of internal heat generation and is expressed by Equation 8. In this equation, $\Delta H_r$

**TABLE 1** Summary of properties of biomass.

| Property | Unit | Material | Value | References |
|---|---|---|---|---|
| Bulk density | kg/m$^3$ | Bark, 49% MC | 295 | 25 |
| | | Bark, loose, wet | 205 | 25 |
| | | Bark, compacted | 318 | 25 |
| | | Woodchips | 210–300 | 27 |
| | | Biomass pellets | 626–742 | 26 |
| Bulk heat capacity | J/kg/K | Bark | 1593 | 25 |
| | | Woodchips | 1350–1500 | 27 |
| | | Biomass pellets | 1366–1463 | 26 |
| Bulk thermal conductivity | W/m/K | Bark | 0.066 | 25 |
| | | Bark | 0.055–0.074 | 28 |
| | | Bark, 12% MC | 0.061–0.0765 | 29 |
| | | Bark, 14%–40% MC | 0.0652–0.1120 | 29 |
| | | Wood | 0.128–0.186 | 28 |
| | | Woodchips (~2 mm) | 0.069 | 27 |
| | | Woodchips (~10 mm) | 0.188 | 27 |
| | | Biomass pellets | 0.142–0.160 | 26 |
| Activation energy | kJ/mol | Bark | 97 | 25 |
| | | Wood | 134 | 25 |
| | | Woodchips | 97–104 | 27 |
| | | Biomass pellets (IMC) | 56–94 | 26 |
| | | Biomass pellets (basket heating) | 75–118 | 26 |
| | | Softwood pellets | 56 | 30 |
| Pile size | m × m × m | Bark (<22 mm) | 84 × 25 × 6 | 25 |
| | | Bark (45–200 mm) | 45 × 12 × 5.5 | 31 |
| | | Woodchips (~10 mm) | 20 × 15 × 6 | 27 |
| | | Woodchips (~2 mm) | 20 × 15 × 5 | 27 |
| | | Woodchips (8–45 mm) | 45 × 12 × 5.5 | 31 |
| Heat of reaction | J/g | Biomass pellets | 40[a] | 21 |
| Peak thermal power | W/g | Biomass pellets | 0.1–1.1 at 60°C | 21 |
| | | Bark | 0.1–0.5 at 50°C[b] | –[c] |

Abbreviation: MC, moisture content.

[a] Estimated from data given in the reference.

[b] As a rule of thumb, the peak thermal power doubles for every temperature increase by 10°C.

[c] Internal, unpublished data.

denotes the heat of reaction, which is assumed to be independent of the extent of reaction.

$$\dot{q}_r = \Delta H_r \cdot A e^{\frac{-E_a}{RT}} \cdot f(\alpha) \tag{8}$$

The mathematical model assumes an isotropic and homogenous material and is primarily selected to study the impact of different reaction models on self-heating. Therefore, the model does not take all affecting conditions into consideration. Such conditions are the stack effect, vaporization of volatile components, and mass transport limitations. Furthermore, it was assumed that the heat capacity and heat conductivity were independent with respect to the extent of the reaction.

## 3 | MATERIALS AND METHODS

### 3.1 | Estimation of $T_{max}$ from simulations

The heat balance equation (Equation 7) was solved by MATLAB using Taylor series expansion and the finite difference method. The highest temperature of the pile was calculated for every timestep. Afterwards, the maximum temperature in the pile ($T_{max}$) over the time interval was calculated. The initial temperature of the pile was set to the same value as the ambient temperature, that is, 20°C. Furthermore, as a conservative approach, the ground was assumed to be well insulating and heat losses through the ground were assumed to be negligible. This resulted in $T_{max}$ always being in the centre of the pile, next to the

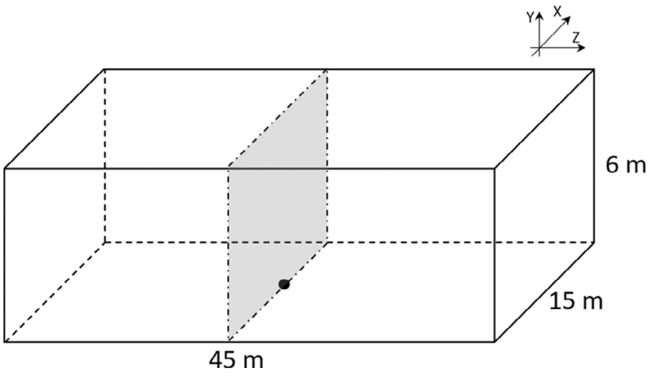

**FIGURE 2** A schematic drawing of the generic pile. The cross-section represents the studied area.

**TABLE 2** Summary of the parameters evaluated in the six different cases.

| Parameter | $\Delta H_r$ | $E_a$ | $HRR_{max}$[a] | $\lambda$ | Pile size |
|---|---|---|---|---|---|
| Unit | J/g | kJ/mol | mW/g | W/m K | $m^3$ |
| Case 1 | 80 | 97 | 0.25 | 0.110 | 45 × 15 × 6 |
| Case 2 | 80 | 97 | 1.0 | 0.110 | 45 × 15 × 6 |
| Case 3 | 100 | 97 | 0.25 | 0.110 | 45 × 15 × 6 |
| Case 4 | 80 | 72.75 | 0.25 | 0.110 | 45 × 15 × 6 |
| Case 5 | 80 | 97 | 0.25 | 0.1375 | 45 × 15 × 6 |
| Case 6 | 80 | 97 | 0.25 | 0.110 | 25 × 10 × 4 |

*Note*: The four reaction models were evaluated four each of the cases.
[a] $HRR_{max}$ at 60°C.

ground. This location is indicated by the black dot in Figure 2. The initial and boundary conditions were set to:

Initial condition:

$$T(x,y)_{t=0} = 20 \tag{9}$$

Boundary conditions:

$$T(0,y) = T(15,y) = T(x,6) = 20 \tag{10}$$

$$\left.\frac{\partial T}{\partial x}\right|_{x=0} = 0 \tag{11}$$

### 3.2 | Reaction model and physical parameters' impact on $T_{max}$

To investigate how the reaction model, as well as some physical parameters impact the maximum temperature in the pile, simulations were performed; the four reaction models were all evaluated in six different cases (cf. Table 2). In each of the cases, $T_{max}$ and the time to reach $T_{max}$ were determined. In the first case, which could be referred to as the base case, the parameters presented in Section 2 were used. In the second case, the specific peak thermal power was increased by four times to 1.0 mW/g (at the reference temperature, 60°C). The change in peak thermal power was made to investigate if the recommendation by Larsson et al.[22] (ranking of material's reactivity based on $HRR_{max}$) could be generalized also to biomass piles. In Cases 3–5, the heat of the reaction was increased by 25%, the apparent activation energy was lowered by 25%, and the heat conductivity was increased by 25%, respectively. Case 6 was similar to the base case, but the size of the pile was reduced. All values were selected based on the literature review (cf. Table 1) and internal experience. All values were judged to be realistic.

The thermal power and total heat versus time for the different reaction models and with the different input values ($\Delta H_r$ and $HRR_{max}$) were calculated (at a constant temperature, 60°C), and the result is presented in Figure 3. The figure exemplifies typical results from isothermal calorimetric measurements. In the figure, it can be seen that time to peak thermal power varied between 0 h and 128 h. The peak thermal power is either 0.25 mW/g or 1.0 mW/g at 60°C and the time to reach 40 J/g varied between 11 and 116 h.

## 4 | RESULT AND DISCUSSION

### 4.1 | $T_{max}$—Maximum pile temperature

The maximum temperatures obtained from simulations of the six different cases with the four reaction models are presented in Figure 4. In the current simulations, the calculated $T_{max}$ is calculated without secondary reactions. This means that $T_{max}$ will be restricted by the heat of the reaction and complete run-away reactions will not be predicted by the model. Instead, it is suggested to interpret the result as the higher $T_{max}$, the higher the risk of secondary reactions, as elaborated, for example, by Graveus and Sutinen.[34]

With Case 1 as the base case, $T_{max}$ varies between 72 and 75°C for the different reaction models, that is, the impact of the reaction model on $T_{max}$ is relatively small. However, a tendency for higher $T_{max}$ is seen for reaction models with thermal powers concentrated around the peak thermal power (e.g., RM1).

In the second case, $HRR_{max}$ was increased by four times, from 0.25 to 1.0 mW/g. Based on previous work and conclusions by Larsson et al.,[21,22] $HRR_{max}$ was expected to have a significant impact on $T_{max}$, as predicted by the model. In this study, the increase in $HRR_{max}$ was found to only have a minor impact on $T_{max}$; $T_{max}$ increased by only between 0.2 and 1.7°C for the different reaction models. A likely reason for this is the relatively low thermal conductivity of the material in combination with the relatively large size of the pile (even with Case 5, the pile is in relative terms large). This results in heat losses much lower than the heat production, even in the case with the lower peak thermal power. If the pile size is reduced, the difference between different peak thermal powers is expected to become more pronounced. This expectation is supported by simulations made with RM1, a pile size of 25 × 4 × 2 m and peak thermal powers of 0.25 and 1.0 mW/g. For the peak thermal powers of 0.25 and 1.0 mW/g,

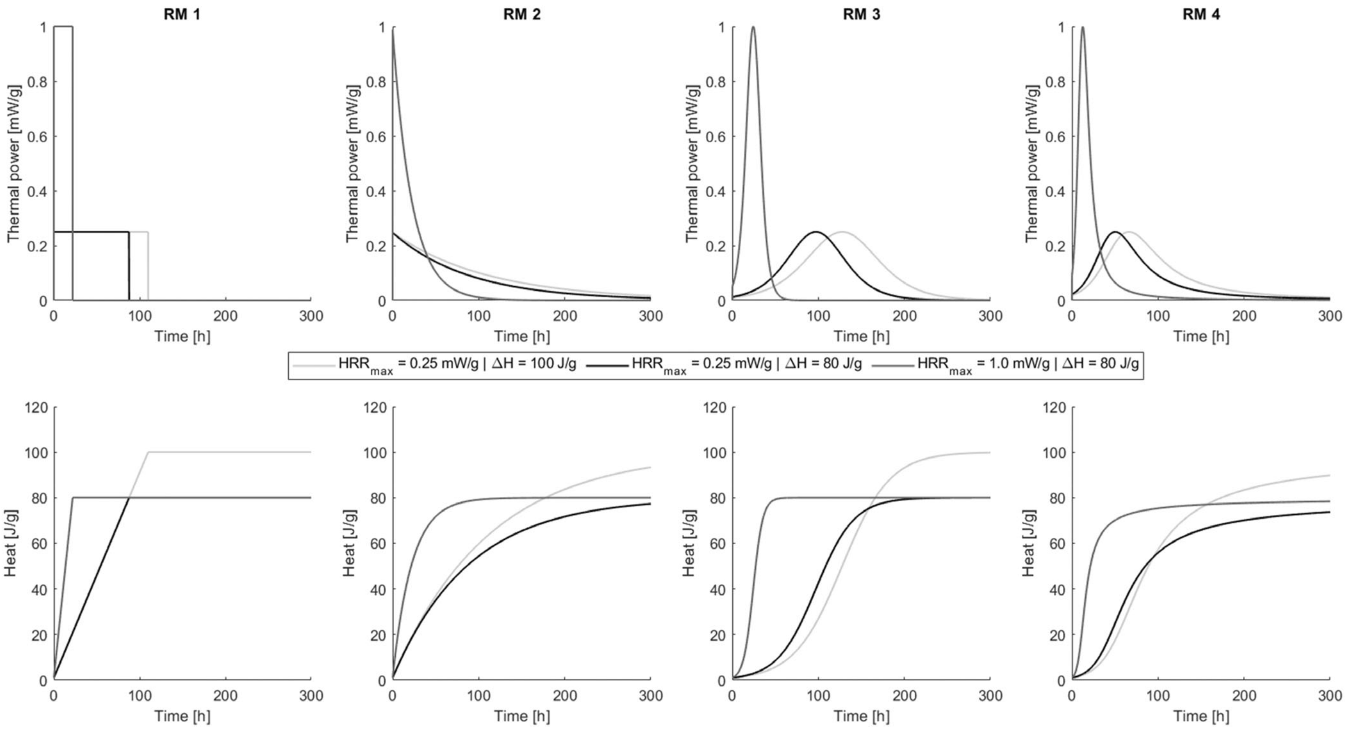

**FIGURE 3** Thermal power and total heat (at 60°C) versus time for the different reaction models and with the different input values ($\Delta H_r$ and $HRR_{max}$). The plots can be seen as examples of results from isothermal calorimetric measurements.

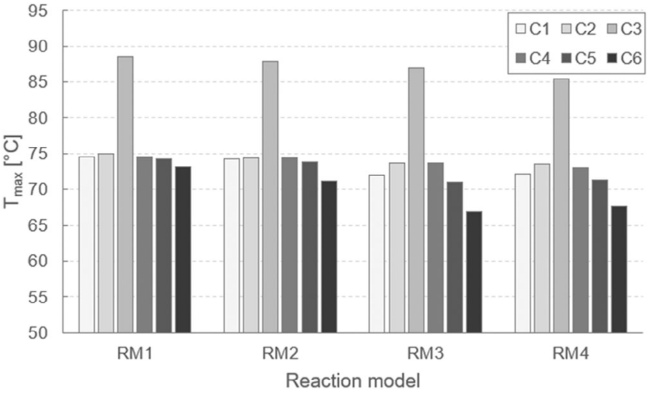

**FIGURE 4** Maximum temperatures for the different cases (C) and with the different reaction models (RM).

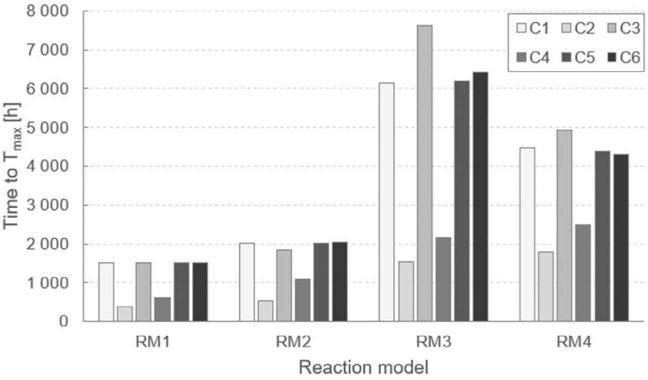

**FIGURE 5** Times to $T_{max}$ for the different cases (C) and with the different reaction models (RM).

$T_{max}$ was calculated to 51.5 and 73.0°C, respectively (which should be compared to 74.5 and 75.0°C in Cases 1 and 2, respectively).

In the third case, that is, an increase in the heat of reaction (total heat released) from 80 to 100 J/g yielded the most significant increase in $T_{max}$; the maximum pile temperature increased by 12 to 14°C, compared to the base case. This finding indicates the importance of accurately measuring the heat of reaction and: (1) never stop isothermal calorimetric measurements before the reaction is completed, and (2) ensure a surplus of oxygen in the ampoule during isothermal calorimetric measurements, that is, the reaction should not be limited by oxygen depletion. This is further demonstrated in Figure 3, especially with reaction Model 2; the curves with the same peak thermal power, but different heat of reactions, almost overlap each other but results in different $T_{max}$ (74.2 and 87.8°C in Cases 1 and 3, respectively).

In the fourth case, the apparent activation energy was lowered. This, however, had almost no impact on $T_{max}$. As has been discussed, it is assumed that the heat losses are relatively small, and the heat of reaction is the governing factor in terms of $T_{max}$. The same conclusions could also be applied to Cases 5 and 6. However, Case 6 illustrates that $T_{max}$ will be lower than for larger piles. This could be used as a mean to control self-heating and thereby reduce material losses and lower the risk of self-ignition.

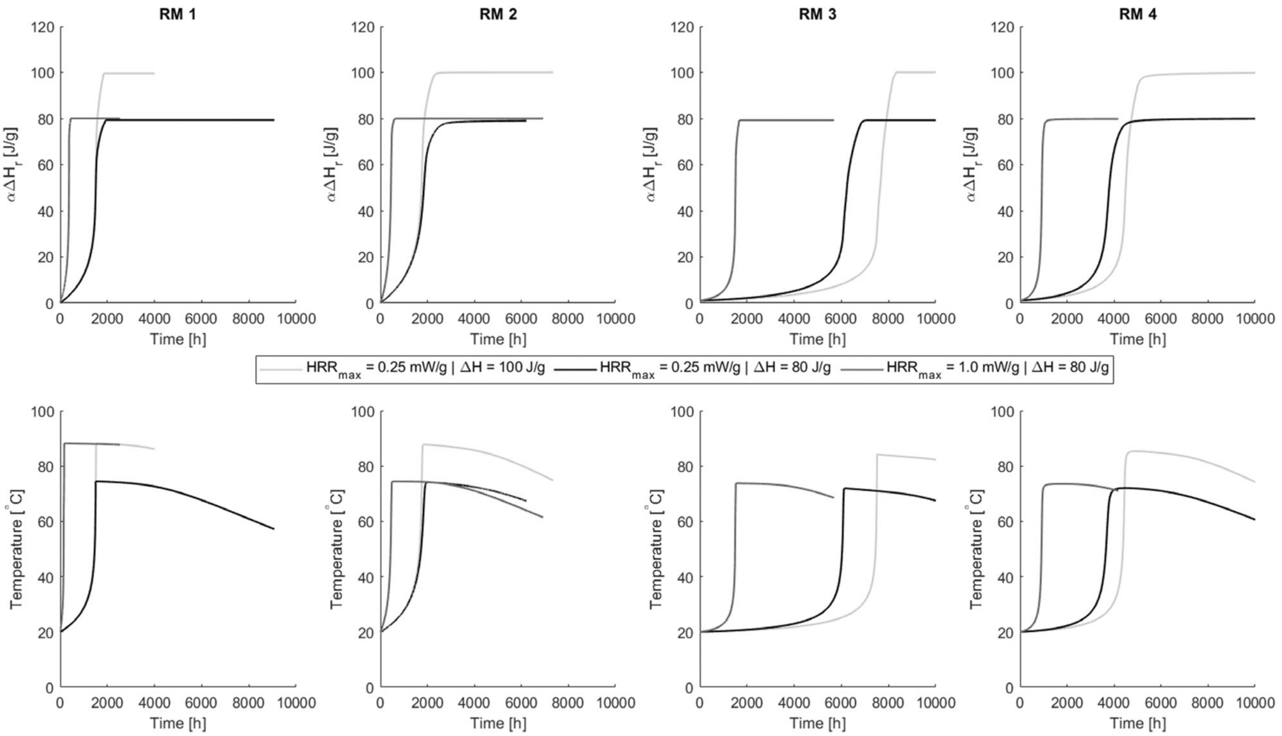

**FIGURE 6** Degree of reaction (material loss) expressed as aΔH$_r$ maximum temperature ($T_{max}$) development in the generic pile versus time.

## 4.2 | Time to $T_{max}$, safe storage time, and reaction progress

Times to $T_{max}$ for the different cases and with the different reaction models is presented in Figure 5. While the differences in $T_{max}$ were found to be relatively small when the different reaction models were compared, the calculated times to reach $T_{max}$ differed significantly; the times ranged from 1510 h (~63 days) to 7630 h (~318 days), depending on case and reaction model. The results indicate a correlation between the peak thermal power, as revealed by isothermal calorimetry, and time to $T_{max}$. In addition, the result also shows that time to $T_{max}$ decreases when the apparent activation energy decreases. In both cases, the findings could be understood; a higher thermal power or earlier peak thermal power should heat the pile faster and thereby shorten the time to $T_{max}$.

When the heat of reaction was increased, that is, in Case 3, time to $T_{max}$ either increased or decreased. This depended on the response of the reaction model on the increase of total heat released (with the peak thermal power kept constant). With RM1 and RM2, the reaction models with the two different heat of reactions almost overlapped, and times to $T_{max}$ changed only marginally. With RM3 and RM4, the peak thermal power was shifted toward later times (cf. Figure 3), which was also reflected by longer times to $T_{max}$.

$T_{max}$ and the reaction progress (expressed as $\alpha \Delta H$) versus time, for Cases 1–3 is given in Figure 6. The figure indicates a relationship between the maximum temperature in the pile and the progress of the current reaction; at higher temperatures, more material has reacted. From the figure, it could be noted when $T_{max}$ exceeds approximately 21°C or 24°C for HRR$_{max}$ equal to 1.0 or 0.25 mW/g, respectively, the temperature increases rapidly (watershed temperature). This tipping point is undesired since the temperature increase results in rapid material losses as well as increases the risk of secondary reactions and self-ignition.

With the peak thermal power and heat of reaction constant, only varying the reaction model, the time to $T_{max}$ changed from 1510 h (RM1, Case 1) to 6130 h (RM3, Case 1). With the reaction models as the only thing differing, this exemplifies the impact of the reaction model on relatively safe storage times, or times when material losses still are relatively small.

## 5 | CONCLUDING REMARK

The impact on $T_{max}$ and time to $T_{max}$ was investigated for six different cases and four different reaction models. The result shows that the total heat released, among the studied parameters, has the largest impact on $T_{max}$; $T_{max}$ increases if the total heat released increases. Peak thermal power has a low impact on $T_{max}$, because of the relatively large sizes of the piles, making them well insulating. Instead, the peak thermal power and the reaction model affect the time to $T_{max}$, that is, the time a material can be stored with less material losses and lower risk of secondary reactions and further self-heating. Furthermore, it was identified that the lower the peak thermal power, the higher the watershed temperature.

### ACKNOWLEDGMENTS

The authors would like to acknowledge AFA Försäkring for the financial support to develop the mathematical model and the Swedish

Energy Agency, as well as the Swedish forest sector, who provided material and covered the cost for the data given in Figure 1.

## CONFLICT OF INTEREST STATEMENT

The authors declare no conflicts of interest.

## DATA AVAILABILITY STATEMENT

The data that support the findings of this study are available from the corresponding author upon reasonable request.

## ORCID

*Sixten Dahlbom* https://orcid.org/0000-0001-9432-0264

## REFERENCES

1. Krigstin S, Wetzel S. A review of mechanisms responsible for changes to stored woody biomass fuels. *Fuel*. 2016;175:75-86. doi:10.1016/j.fuel.2016.02.014
2. He X, Lau AK, Sokhansanj S, Jim Lim C, Bi XT, Melin S. Dry matter losses in combination with gaseous emissions during the storage of forest residues. *Fuel*. 2012;95:662-664. doi:10.1016/j.fuel.2011.12.027
3. Jirjis R. Storage and drying of wood fuel. *Biomass Bioenergy*. 1995; 9(1):181-190. doi:10.1016/0961-9534(95)00090-9
4. Jylhä P, Hytönen J, Alm J. CO2 release and dry matter loss of scots pine forest chips stockpiled from late summer to winter. *Biomass Bioenergy*. 2017;104:36-44. doi:10.1016/j.biombioe.2017.06.003
5. Thörnqvist T. Drying and storage of forest residues for energy production. *Biomass*. 1985;7(2):125-134. doi:10.1016/0144-4565(85)90038-1
6. Chang Y, Hudson HJ. The fungi of wheat straw compost: I. Ecological studies. *Transactions of the British Mycological Society*. 1967;50(4): 649-666. doi:10.1016/S0007-1536(67)80097-4
7. Pari L, Brambilla M, Bisaglia C, et al. Poplar wood chip storage: effect of particle size and breathable covering on drying dynamics and biofuel quality. *Biomass Bioenergy*. 2015;81:282-287. doi:10.1016/j.biombioe.2015.07.001
8. Anerud E, Larsson G, Eliasson L. Storage of wood chips: effect of chip size on storage properties. *Croatian Journal of Forest Engineering*. 2020;41:11. doi:10.5552/crojfe.2020.663
9. Baadsgaard-Jensen J. Storage and Energy Economy of Chunk and Chip Piles. Report No. STEV-TB-91-27; CONF-8812164-Vol.2; SLU-ISK-U-134-88 1988.
10. Anerud E, Bergström D, Routa J, Eliasson L. Sieving and covering of wood chips improves storability. *Energies*. 2022;15(8):2953. doi:10.3390/en15082953
11. Afzal MT, Bedane A, Shahab S, Waseem M. Storage of comminuted and uncomminuted forest biomass and its effect on fuel quality. *BioResources*. 2010;5:55-69.
12. Manzone M, Balsari P, Spinelli R. Small-scale storage techniques for fuel chips from short rotation forestry. *Fuel*. 2013;109:687-692. doi:10.1016/j.fuel.2013.03.006
13. Wetzel S, Volpe S, Damianopoulos J, Krigstin S. Can biomass quality Be preserved through tarping comminuted roadside biomass piles? *Forests*. 2017;8(9):305. doi:10.3390/f8090305
14. Anerud E, Bergström D, Routa J, Eliasson L. Fuel quality and dry matter losses of stored wood chips—influence of cover material. *Biomass Bioenergy*. 2021;150:106109. doi:10.1016/j.biombioe.2021.106109
15. Alakoski E, Jämsén M, Agar D, Tampio E, Wihersaari M. From wood pellets to wood chips, risks of degradation and emissions from the storage of woody biomass – a short review. *Renew Sustain Energy Rev*. 2016;54:376-383. doi:10.1016/j.rser.2015.10.021
16. Arshadi M, Geladi P, Gref R, Fjällström P. Emission of volatile aldehydes and ketones from wood pellets under controlled conditions. *Ann Occup Hyg*. 2009;53(8):797-805. doi:10.1093/annhyg/mep058
17. Arshadi M, Gref R. Emission of volatile organic compounds from softwood pellets during storage. *For Prod J*. 2005;55:132-135.
18. Arshadi M, Tengel T, Nilsson C. Antioxidants as additives in wood pellets as a mean to reduce off-gassing and risk for self-heating during storage. *Fuel Process Technol*. 2018;179:351-358. doi:10.1016/j.fuproc.2018.07.026
19. Persson H, Leandersson A, Piku Amen M, Lönnermark A. Lagring av biobränsle och avfall: Statistik och erfarenheter från incidenter och bränder. 2014. SP Rapport 2014:55. 978-91-87461-98-9 (ISBN) http://urn.kb.se/resolve?urn=urn:nbn:se:ri:diva-5210
20. Lönnermark A, Persson H, Trella F, Blomqvist P, Boström S, Bergérus RÅ. Brandsäkerhet vid lagring av avfallsbränslen. 2018:89. Avfall Sverige. 11034092 (ISSN). 2018 http://urn.kb.se/resolve?urn=urn:nbn:se:ri:diva-39949
21. Larsson I, Lönnermark A, Blomqvist P, Persson H, Bohlén H. Development of a screening test procedure based on isothermal calorimetry for determination of self-heating potential of biomass pellets. *Fire Mater*. 2017;41(8):940-952. doi:10.1002/fam.2427
22. Larsson I, Lönnermark A, Blomqvist P, Persson H. Measurement of self-heating potential of biomass pellets with isothermal calorimetry. *Fire Mater*. 2017;41(9):1007-1015. doi:10.1002/fam.2441
23. Pushp M, Lönnermark A, Hedenqvist M, Vikegard P. Heat production in municipal and industrial waste as revealed by isothermal microcalorimetry. *J Therm Anal Calorim*. 2021;147:8271-8278. doi:10.1007/s10973-021-11117-2
24. International Organization for Standardization. Solid biofuels—determination of self-heating of pelletized biofuels—part 1: isothermal calorimetry. 2020. 38. (ISO 20049-1:2020).
25. Krigstin S, Helmeste C, Jia H, et al. Comparative analysis of bark and woodchip biomass piles for enhancing predictability of self-heating. *Fuel*. 2019;242:699-709. doi:10.1016/j.fuel.2019.01.056
26. Larsson I, Sjöström J, Lönnermark A, Andersson J, Persson H, Blomqvist P. Deliverable D4.3: report on Matematical Modelling, Including Input Parameters. Report No. Project manager BIOENERGY2020+ GmbH; Scientific partner SP Technical Research Institute of Sweden; 2014.
27. Ferrero F, Lohrer C, Schmidt BM, Noll M, Malow M. A mathematical model to predict the heating-up of large-scale wood piles. *Journal of Loss Prevention in the Process Industries*. 2009;22(4):439-448. doi:10.1016/j.jlp.2009.02.009
28. Raznjevic K. *Handbook of Thermodynamic Tables and Charts*. Hemisphere Publishing Corporation; 1976.
29. Pásztory Z, Ronyecz I. The thermal insulation capacity of tree bark. *Acta Silv et Lignaria Hungarica*. 2013;9:111-117. doi:10.2478/aslh-2013-0009
30. Guo W, Trischuk K, Bi X, Lim CJ, Sokhansanj S. Measurements of wood pellets self-heating kinetic parameters using isothermal calorimetry. *Biomass Bioenergy*. 2014;63:1-9. doi:10.1016/j.biombioe.2014.02.022
31. Anerud E, Eriksson A. Evaluation of an improved design for large-scale storage of wood chip and bark. *Biomass Bioenergy*. 2021;154: 106255. doi:10.1016/j.biombioe.2021.106255
32. Ng W. Thermal decomposition in the solid state. *Aust J Chem*. 1975; 28(6):1169-1178. doi:10.1071/CH9751169
33. Özilgen S, Özilgen M. Kinetic model of lipid oxidation in foods. *J Food Sci*. 1990;55(2):498. doi:10.1111/j.1365-2621.1990.tb06795.x
34. Graveus F, Sutinen A. *Analys av riktlinjer för utomhuslagring av trädbaserat biobränsle till kraftvärmeverk*. Department of Fire Safety Engineering. Report no. 5473. 2015.

**How to cite this article:** Dahlbom S, Anerud E, Lönnermark A, Pushp M. A theoretical evaluation of the impact of the type of reaction on heat production and material losses in biomass piles. *Fire and Materials*. 2023;47(8):1074-1081. doi:10.1002/fam.3153